Electronic Supplementary Material (ESI) for RSC Advances.

Supporting information for "Antimony tin oxide porous layer improve poly(3,4-ethylenedioxythiophene) counter electrode fabricated by vapor deposition for dye-sensitized solar cell"

Xiang Xia,[a] Wenyi Wu,[b] Jiahui Ma,[b] Tingting Liu,[b] Dehou Fei ,[a] Xizhe Liu*[a] and Chunxiao Gao[b]

[a]*Laboratoryfor Applied Atomic and Molecular Spectroscopy, Institute of Atomic and Molecular Physics, Jilin University, Changchun 130012, P. R. China.*
[b]*State Key Laboratory for Superhard Materials, Jilin University, Changchun 130012, P. R. China.*

**Corresponding author.*
Fax: 8643185168816; Tel: 8643185168817
E-mail: liu_xizhe@jlu.edu.cn (Xizhe Liu)

1. Preparation and fabrication of Dye sensitized solar cells (DSSCs)

1.1. Preparation of 2,5-Dibromo-3,4-ethylenedioxythiophene (DBEDOT)

DBEDOT was prepared as previews work[1] with a little change. 3,4-ethylenedioxythiophene (EDOT) (3.0 g, 0.021 mol) was dissolved in amixture solvent of 50 ml chloroform and 50 ml acetic acid. Then, *N*-bromosuccinimide (8.0 g, 0.045 mol) was added at 0-5 °C under nitrogen atmosphere in the mixture solution. This mixture was stirred strongly for 2.5 h at room temperature before 200 ml water was added in it. The mixture divided into water layer and organic layer and the organic layer was extracted with separatory funnel. Then, the organic layer was neutralized with 5% sodium bicarbonate solution, and washed with distilled water for 3 times. Finally, crude powder was got by distillation, and this crude powder was recrystallized from boil ethanol to produce white crystals.

1.2. Preparation of porous ATO supporting layers

ATO nanoparticle was purchased from Aladdin Reagent. ATO nanoparticle, terpineol, ethyl cellulose, lauric acid and ethanol were mixed uniformly with a mass ratio of 1.0 : 6.0 : 0.3 : 0.1 : 15 to get the ATO nanoparticle paste. Firstly, ethyl cellulose and lauric acid were dissolved in terpineol, this mixture was stirred at 80 ^{o}C for 12 h. Then, this mixture was added into an ATO nanoparticle solution, which was prepared by dispersing the ATO nanoparticle into ethanol by sonication. Finally, the ATO mixture was ball milled for 12 hours to get the ATO nanoparticle paste.

400 ul ATO nanoparticle paste was diluted to 1400 ul by ethanol as paste solution A, and the original ATO nanoparticle paste as paste solution B. Partial coverage ATO layer, 100 nm ATO layer and 200 nm ATO layer were obtained by spin coating paste solution A at 6000 rpm, 4000 rpm and 2000 rpm for 60 sec, respectively. 500 nm ATO layer was obtained by spin coating paste solution B at 2000 rpm for 60 sec. The samples were sintered at 450 ^{o}C for 20 min to get the porous ATO supporting layers.

1.3. Fabrication of DSSCs

PEDOT electrodes and PEDOT/ATO composite electrodes were fabricated by vapor deposition method. Briefly, fluorine doped tin oxide (FTO) glasses were cleaned and ATO nanoparticle paste solution were deposited by spin coating. Then, the samples were sintered at 450 ^{o}C for 20 min to get the porous supporting layer. Then, 50 mg DBEDOT was placed in a 100 ml closed vessel with substrates together. PEDOT were deposited on two kinds of substrates, bare FTO and FTO with ATO porous film. The system was purged with nitrogen and pumped (about 1000 Pa) before placed in an oven at 70 ^{o}C for 3 hours. The influence of different deposition time (1 hour, 2 hours, 3 hours and 6 hours) was also studied. Then, blue PEDOT film was produced on the substrates. Finally, the PEDOT film was treated with 0.5 M $LiClO_4$ in acetonitrile solution for 12 h. Pt electrodes were prepared by spin coating of 0.02 M H_2PtCl_6 in ethanol solution and sintered at 380 ^oC for 30 min.

TiO_2 working photoanodes were prepared on FTO substrates by doctor blade technique. The samples were dried and sintered at 80 ^oC for 20 min, 125 ^oC for 20 min, 325 ^oC for 20 min, and 490 ^oC for 20 min. After further treatment with 40 mM $TiCl_4$ at 70 ^oC, the porous TiO_2 films were rinsed with water and ethanol, and sintered at 450 ^oC for 30 min. Once cooling to 80 ^oC, the TiO_2 electrodes were immersed into the 0.5 mM N719 dye solution for 24 h in the dark, while the solvent was 1/1 (v/v) mixture of acetonitrile and tert-butanol. The electrolyte was composed of 0.1 M LiI, 0.05 M I_2, 0.6 M 1-methyl-3-propylimidazolium iodide and 0.5 M tert-butylpyridine in acetonitrile solution. The CEs were assembled with the prepared TiO_2 photoanodes in sandwich structure to get the solar cell devices.

1.3. Characterization

The X-ray diffraction (XRD) spectra were obtained using a Bruker D8 Advance X-ray diffractometer with Cu Kα radiation (λ=1.5418 Å). The surface morphologies (Fig. 1) were investigated by JSM 6700F Scanning Electron Microscope (SEM). Energy Disperse Spectroscopy (EDS) and the SEM images (Fig. S3) were investigated by FEI MAGELLAN 400 Scanning Electron Microscope. Photocurrent density-photovoltage characteristics were recorded by a CHI660D electrochemical workstation and a solar simulator. The active area of DSSCs was 0.15 cm^2, which defined by a mask. The

AM1.5 illumination was provided by a solar simulator (ABB class, NBet Co.Ltd.), which was calibrated to 100 mWcm^{-2} by a Si reference solar cell. Electrochemical impedance spectra of dummy cells, which were composed of two identical electrodes and the same electrolyte used in devices, were recorded over a frequency range of 100 kHz to 0.1 Hz by CHI660D electrochemical workstation. The bias voltage and perturbation amplitude was 0 mV and 10 mV, respectively, and the effective area was 0.25 cm^2. The cyclic voltammograms were measured with a three-electrode system, that the prepared CEs were used as the working electrode, Pt wire as the counter electrode and Ag/AgCl as the reference electrode. The electrolyte was composed of 0.1 M $LiClO_4$, 0.01 M LiI and 0.001 M I_2 in acetonitrile solution.

2. Energy Disperse Spectroscopy (EDS)

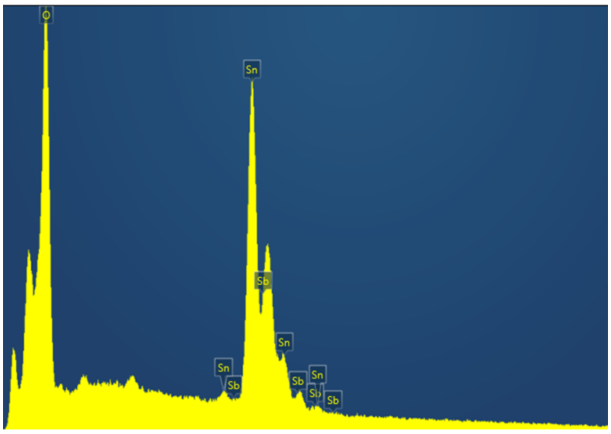

Fig. S1 Energy Disperse Spectroscopy of the ATO film

Table S1 Weight percent (wt%) of the element obtained from EDS.

Element	wt%
O	25.96
Sn	65.34
Sb	8.70
Total:	100.00

3. Electrochemical impedance spectra of the DSSCs

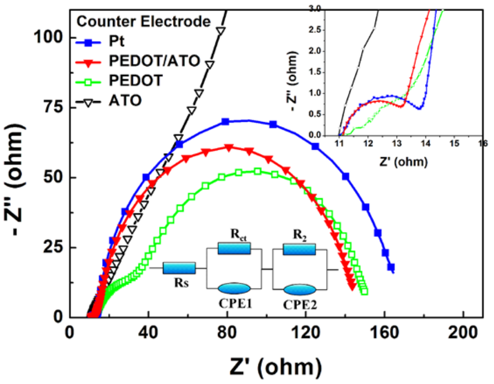

Fig. S2 Electrochemical impedance spectra (EIS) of the DSSCs based on Pt electrode, PEDOT/ATO composite electrode, PEDOT electrode, and ATO electrode. Up-right insert figure is the enlargement of high frequency impedance, and another insert figure is the equivalent circuit model.

Table S2 Impedance Parameters of DSSCs with Various CEs.

Counter electrode	$R_s(\Omega)$ [a]	$R_{ct}(\Omega)$ [b]	$R_2(\Omega)$ [c]	CPE_1-T[d] (10^{-4})	CPE_1-P[e]	CPE_2-T[f] (10^{-4})	CPE_2-P[g]
Pt	11.1	2.97	152	1.08	0.72	8.06	0.95
PEDOT/ATO	11.0	2.34	134	1.31	0.74	8.69	0.91
PEDOT	14.0	28.92	107	3.24	0.74	6.27	0.97
ATO	-	-	-	-	-	-	-

[a] the series resistance.

[b] the charge transfer resistance at the counter electrode/electrolyte interface.

[c] the charge transfer resistance at the TiO_2/electrolyte interface.

[d, e] The two values define the constant phase element at the counter electrode/electrolyte interface.

[f, g] The two values define the constant phase element at the TiO_2/electrolyte interface.

Fig. S2 shows the EIS of the DSSCs based on different CEs. With the equivalent circuit model, we fit the EIS and obtain the parameters, which are summarized in Table S2. It was recorded over a frequency range of 100 kHz to 0.1 Hz by CHI660D electrochemical workstation in dark. The bias voltage and perturbation amplitude is 700 mV and 10 mV, respectively, and the effective area is 0.35 cm^2. In Fig. S2, the arches demonstrate the charge transfer process and diffusion process in DSSCs. As previous reports[2-4], the high-frequency feature (the enlarged figure in Fig. S2) is attributed to the charge transfer resistance (R_{ct}) at the counter electrode/electrolyte interface.

For PEDOT/ATO composite electrode, the charge transfer resistance at the counter electrode/electrolyte interface is 2.34 Ω (0.35 cm^2), which is much smaller than that of PEDOT electrode (28.92 Ω, 0.35 cm^2). This confirms that PEDOT/ATO composite electrode exhibits higher electrocatalytic activity than PEDOT electrode in the completed DSSC device. Considering the electrode areas, the difference of charge transfer resistance per unit area for PEDOT/ATO electrode or PEDOT electrode is less than 7% in two separate EIS measurements (in dummy cells or in completed DSSC devices).

4. SEM images

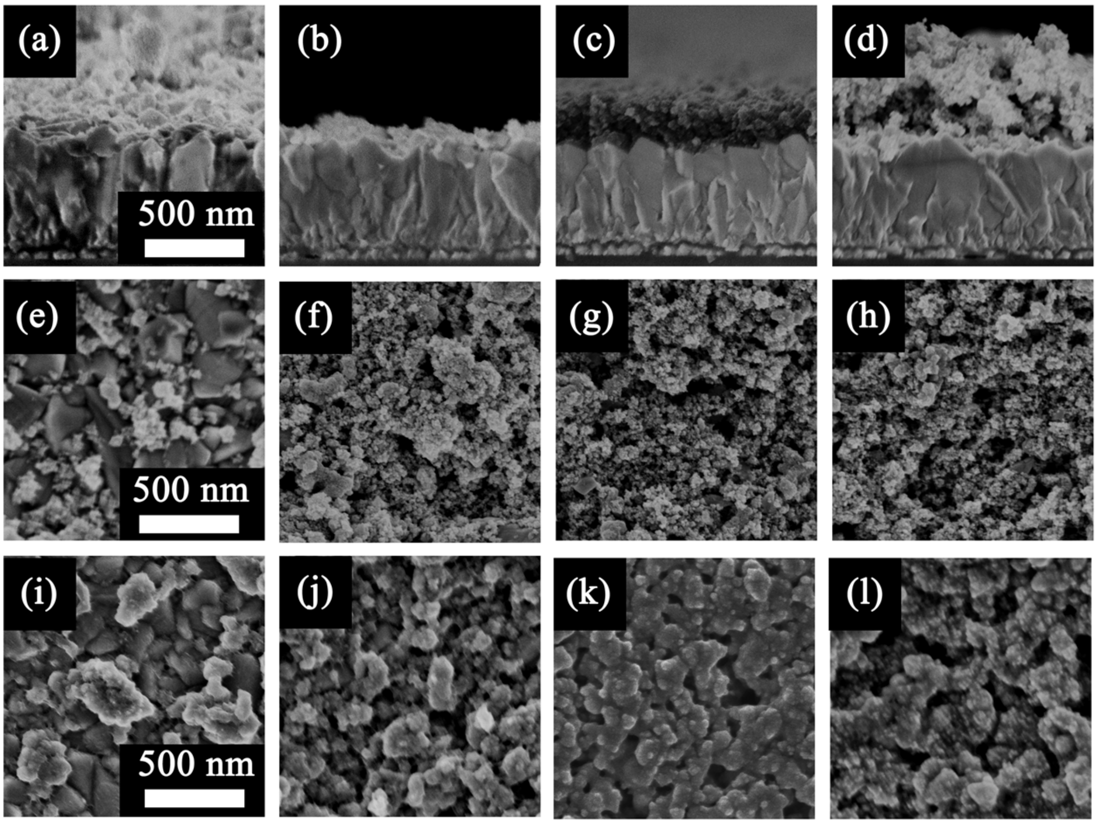

Fig. S3 (a), (b), (c) and (d) are cross section images of ATO supporting layers with different thickness. (e), (f), (g) and (h) are surface morphology images of ATO supporting layers with different thickness. (i), (j), (k) and (l) are surface morphology images of PEDOT/ATO composite electrodes with different ATO layer thickness. The SEM images in the same column share the same ATO supporting layer.

5. Photocurrent density-photovoltage curves

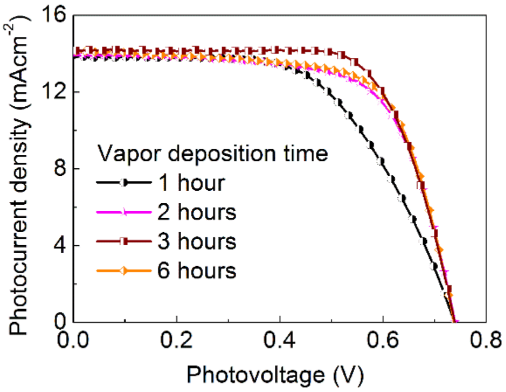

Fig. S4 Photocurrent density-photovoltage curves of DSSCs under 100 mWcm^{-2} AM 1.5G illumination, which are fabricated with PEDOT/ATO composite electrodes with different vapor deposition time. The deposition temperature is 70 °C and 200 nm ATO layers are used as the supporting layers.

Table S3 Photovoltaic parameters of DSSCs with PEDOT/ATO composite electrodes based on different vapor deposition time.

Vapor deposition time	V_{oc} (V) [a]	J_{sc} (mAcm^{-2}) [b]	Fill factor	η %[c]
1 hour	0.737	13.8	0.58	5.93
2 hours	0.739	13.9	0.68	6.95
3 hours	0.735	14.3	0.71	7.42
4 hours	0.736	14.1	0.69	7.13

[a] open circuit photovoltage.

[b] short circuit photocurrent density.

[c] solar-to-electric conversion efficiency.

For vapor deposited PEDOT/ATO electrodes, four different deposition times are tested (1 hour, 2 hours, 3 hours and 6 hours). The photocurrent density-photovoltage curves of DSSCs based on these electrodes are shown in Fig. S4, and their photovoltaic parameters are summarized in Table S3. The difference of photovoltaic performance mainly comes from the difference on the fill factors, and the deposition time of 3 hours gives best performance (conversion efficiency is 7.42 %). Short deposition time (1 hour and 2 hours) cannot produce enough PEDOT on the ATO supporting layer, which result in relative low conversion efficiency (5.93 % and 6.95

%, respectively). Further increasing the deposition time to 6 hours also results in a decrease of conversion efficiency (7.13 %). It is because that excessive PEDOT blocks the ion diffusion channel and shows a negative effect on the electrochemical activity of the electrode[5].

6. Electrochemical stability

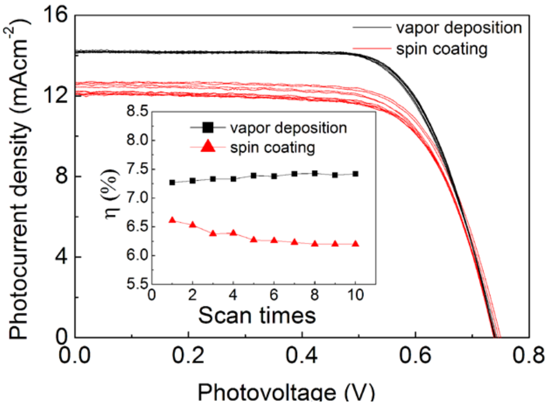

Fig. S5 Photocurrent density-photovoltage curves of DSSCs under 100 mWcm^{-2} AM 1.5G illumination, which is fabricated with vapor deposited PEDOT/ATO composite electrode (black lines) and spin-coated PEDOT electrode (red lines). The devices are scanned ten times to study their electrochemical stability. The relationship between the conversion efficiency (η %) and the scan times are shown in the inset figure, black solid square represents vapor deposited PEDOT/ATO composite electrode and red solid triangle represents spin-coated PEDOT electrode.

The previous report developed a spin-coating method based on the solid state polymerization of 2,5-Dibromo-3,4-ethylenedioxythiophene for fabricating PEDOT electrodes[6]. In their report, the optimized conversion efficiency is 4.9 %. For comparison, we make the spin-coated PEDOT electrode following their optimized condition. We get an initial conversion efficiency of 6.61% by this spin-coated electrode, and the efficiency decreases to 6.20 % after 10 times repeated measurements. In the same condition, our vapor deposited PEDOT/ATO electrode can lead to an initial conversion efficiency of 7.27%, which increases to 7.42% after

10 times repeated measurements. Therefore, our vapor deposited PEDOT/ATO electrode has better performance than the spin-coated PEDOT electrode in efficiency and stability.

References

1 H. Meng, D. F. Perepichka, M. Bendikov, F. Wudl, G. Z. Pan, W. J. Yu, W. J. Dong and S. Brown, *J. Am. Chem. Soc.* 2003, **125,** 15151.

2 Q. Wang, J. E. Moser and M. Grätzel, *J. Phys. Chem. B* 2005, **109,** 14945.

3 F. Fabregat-Santiago, J. Bisquert, G. Garcia-Belmonte, G. Boschloo, and A. Hagfeldt, *Sol. Energy. Mat. Sol. C.* 2005, **87,** 117.

4 M. Wu, X. Lin, A. Hagfeldt and T. Ma, *Angew. Chem. Int. Edit.* 2011, **50,** 3520.

5 X. Yin, F. Wu, N. Fu, J. Han, D. Chen, P. Xu, M. He and Y. Lin, *ACS Appl. Mater. Inter.* 2013*,* **5,** 8423.

6 L. Chen, J. Jin, X. Shu and J. Xia, *J. Power. Source* 2014, **248,** 1234.